# A Spatiotemporal Analysis of New York State Grid Transition under the CLCPA Energy Strategy

M. Vivienne Liu
Cornell University
ml2589@cornell.edu

Kenji Doering
Cornell University
kmd266@cornell.edu

Amandeep Gupta
Fluence Energy
Amdeepgup@gmail.com

C. Lindsay Anderson
Cornell University
cla28@cornell.edu

## Abstract

*To decarbonize the energy sector, clean energy plans with a tremendous quantity of renewable energy integration are emerging globally. New York State (NYS) has one of the most ambitious targets to realize carbon-neutrality by 2040. To investigate the feasibility of this plan, the starting point of the plan is analyzed on a modified representation of the NYS power grid. Historical data for 2019 is used to model the spatiotemporal co-variability of load and virtual renewable outputs at hourly intervals. Optimal power flow analysis is simulated on daily basis for the full year to examine the performance of the system from annual to hourly levels. Results identify bottlenecks to using renewable energy efficiently and reliably with an emphasis on storage units, providing system operators, policymakers, and stakeholders with a practical research foundation.*

**Keywords:** Renewable integration, Decarbonization, Battery analysis, Power system modeling

## 1. Introduction

The Paris Agreement states that the global warming increase should be controlled under 2 °C relative to pre-industrial levels, which is recently analyzed in the latest IPCC report [1]. Five illustrative scenarios projecting the global warming levels from very low Greenhouse Gas (GHG) emissions to very high GHG emissions are presented in the report, covering potential temperature increases from 1-8.5 °C. To stay under 2 °C of temperature increase, GHG emissions have to decrease to net-zero around 2050. Electricity and heat accounted for 31.9% of world GHG emissions [2] in 2018. As a result, plans to achieve zero-emission by 2050 have been proposed globally to create a sustainable and reliable future.

An overview of clean electricity policies for the US and some other countries is summarized in [3]. With European countries leading the way and targeting a nearly 100% cut in emissions by 2050, Australia and China plan to achieve 50% and 35% of renewable energy penetration by 2030. In the US, various states or territories have set renewable targets for the next few decades where the New York State (NYS) has one of the most ambitious goals to have 70% of renewable by 2030 ("70 $\times$ 30") and to realize carbon-neutrality by 2040, which is legally bonded by the Climate Leadership and Community Protection Act (CLCPA).

Roadmaps for all 50 states in the US are proposed by [4] at the annual level to foster the implementation of clean energy policies. However, an annual scale analysis underestimates the temporal variabilities of demand and the high intermittent renewable energy. A multi-scale framework that considers capacity planning at hourly resolution is proposed by [5] to examine the transition plan of NYS. Even though the model has high hourly resolution and considers multiple types of generators and storage units, the power grid is simplified as a single node which ignores spatial co-variability. The spatial distributions of load and renewable energy are of great importance, which is especially true for NYS as it has highly imbalanced renewable supply and demand.

The New York Independent System Operator (NYISO) contracted with two analysis groups to study the climate change impact on long-term load (phase-I) [6] and power system reliability (phase-II) [7]. While the phase-I study focuses on long-term load prediction under climate-change impacts and electrification of transportation and heating, the phase-II report investigates the power system reliability

URI: https://hdl.handle.net/10125/102944
978-0-9981331-6-4

**Nomenclature Sets and Indexes**

$T$ length of the planning horizon
$Gn$ total number of generators in the system
$Bn$ total number of buses in the system
$Ln$ total number of branches in the system
$Sn$ total number of storage units in the system
$Ifn$ total number of interfaces in the system
$G_b$ a set of generators connected to bus $b$
$I_b$ a set of lines flow in to bus $b$
$O_b$ a set of lines flow out of bus $b$
$S_b$ a set of storage units connected to bus $b$
$IF_i$ a set of lines in zonal interface $i$
$b \in \{1, ..., Bn\}$ a bus in the system
$t \in \{1, ..., T\}$ a time interval
$g \in \{1, ..., Gn\}$ a generator in the system
$l \in \{1, ..., Ln\}$ a transmission line in the system

**Parameters**

$\overline{R}_g/\underline{R}_g$ upper/lower ramp rate limit of generator $g$
$\overline{P}_g/\underline{P}_g$ generation upper/lower bound of generator $g$]
$\overline{L_l}/\underline{L_l}$ upper/lower bound of transmission line $l$
$\overline{L_{IF_i}}/\underline{L_{IF_i}}$ upper/lower bound of interface flow $i$
$C_{g,t}/C^c_{g,t}$ linear/constant cost coefficient of generator $g$ at time $t$
$D_{b,t}$ demand for bus $b$ in hour $t$
$\eta_s$ round-trip efficiency of the storage unit at bus $s$
$SOC_s$ storage size for storage unit $s$
$\Delta_s$ charging/discharging capacity of storage unit $s$

**Variables**

$p_{g,t}$ generation of generator $g$ in hour $t$
$e_{l,t}$ power flow of branch $l$ in hour $t$
$\theta_{b,t}$ phase angle of bus $b$ in hour $t$
$\delta^+_{s,t}, \delta^-_{s,t}$ charge/discharge power of storage unit $s$ in hour $t$
$soc_{s,t}$ amount of stored energy in the storage unit $s$ at hour $t$

under a resource set with massive wind and solar generation, price responsive demand, and DE resources [1]. The starting point of the resource set is based on the "70 $\times$ 30" scenario developed in the Congestion Assessment and Resource Integration Study [8]. An energy balance model with 11 buses (one for each load zone) is used in the phase-II report to identify the need for DE resources. The analysis also considers the loss of load occurrences, which can be used to identify system vulnerability under climate disruption scenarios. However, the climate disruption scenarios considered in the report are limited to 30-day horizons which fail to capture the seasonal variance. Furthermore, the scenarios that provide predictions for the long-term (to 2040) are not modeled to capture the co-variability of meteorological variables that govern renewable output and drive demand patterns, such as temperature and wind speed. Lastly, the energy balance model oversimplifies the underlying topology of the grid and might potentially underestimate the vulnerability of the system.

It is critical to address the research gaps identified above for the feasibility of the large-scale renewable development proposed in the CLCPA as NYS only had 27% of statewide generation from renewable resources [9] in 2019. In this paper, we take a different approach to investigate the feasibility of the CLCPA plan and address the research gaps mentioned above. Instead of projecting for extreme scenarios in 2040, it is crucial to first assess the ability of the grid to efficiently and reliably dispatch the integrated renewables on a day-to-day basis with the transmission capacity expansion planned for the future. Therefore, the year 2019 is chosen[2] to perform Optimal Power Flow (OPF) analysis for a full year. By using historical data, the spatiotemporal co-variability is well preserved and the analysis can be performed long enough to observe seasonal trends. The open-source NYS grid representation in [10] is used as a baseline, and modified to layout the analysis as it has geographic information embedded in the system and provides validated underlying grid topology of the NYS with spatiotemporal data. Virtual wind and solar sites and storage units are added to the baseline model based on zonal capacities identified as the starting point of the CLCPA plan in the CARIS report [8]. Note that the electrification of the transportation and heating sectors would increase the load and potentially shift it from summer peak to winter peak at around 2034 [11], which is not considered by using the 2019 data. In addition, more extreme events such as droughts, wind lulls, and extreme temperatures could be exacerbated as climate change intensifies, leading to more complicated system

[1]DE resource is a synthetic resource that is assumed to be dispatchable and emission-free. Quantifying the need for the DE resource provides insights on planning for the future grids.

[2]The year 2019 is chosen to avoid the impact of the Covid-19 pandemic.

operation conditions. As a result, 2019 is a milder system condition, which could serve as an upper bound on the feasibility of the CLCPA for the scenarios we are projecting for the future. The major contributions of this paper can be summarized as follows:

- The starting point of the CLCPA plan is integrated into a realistic representation of the NYS grid and optimized with hourly OPF analysis for a full year, to provide more realistic results with higher spatiotemporal resolution.
- Historical data from 2019 is chosen to preserve the spatial-temporal co-variability for renewables and load which depends on meteorological variables.
- Analysis on multiple time scales is performed to study the yearly, seasonally and intra-daily behavior of the system and pinpoint the potential vulnerabilities of the grid under non-extreme operation conditions.
- Special focus is given to the duration and cycling constraints of batteries, which is informative to future investment, allocation, and operation of storage units.

The rest of the paper is organized as follows: Section 2 introduces the baseline model of the NYS grid and the spatiotemporal renewable output modeled based on the resource set in [7]. Section 3 describes the modified OPF model and formulates the problem mathematically. Section 4 designs the test cases to compare the system performances and evaluates the feasibility of the CLCPA plan. Section 5 shows the numerical results from annual overview to intra-day investigation and presents the flexibility provided by batteries. Section 6 concludes the paper and discusses future work directions.

## 2. Data Description

### 2.1. Modified NYS Power Grid

The open-source NYS power grid representation in [10] is used as the grid model for this paper as it has geographic coordinates for the buses and has been validated with both Power Flow and Optimal Power Flow analysis against historical records from the New York Independent System Operator (NYISO). The representation in [10] will be referred to as the "baseline" model throughout the paper as it provides a baseline for the grid status of 2019. Modifications will be made for transmission lines, wind farms, solar farms, and storage units as the CLCPA plan suggests.

The baseline model has 57 buses and 94 transmission lines, where 46 of the buses are for New York and nine are for neighboring areas. There are 227 thermal generators, ten hydro generators, and six nuclear generators being modeled as dispatchable units. Note that one bus can have multiple generators of different fuel types. In addition, 14 wind farms and 18 other renewable generators are modeled as non-dispatchable units (negative load) due to their generation contribution at less than 3% of annual generation for 2019. Linear cost curves are fitted for the thermal generators based on the heat rates of each unit and the dynamics of fuel prices.

There are 11 load zones in NY and the interface flow between each pair of load zones has transmission capacity limits. Load zones and the simplified network between load zones and neighbor grids are shown in Figure 1 The baseline model tracks the dynamic capacity limits from NYISO's records [12]. To test the feasibility of the CLCPA plan, the interface flow capacity limits are fixed as shown in Table 1 referring to the Reliability Needs Assessment (RNA) report [13], which suggests the interface capacity for 2030.

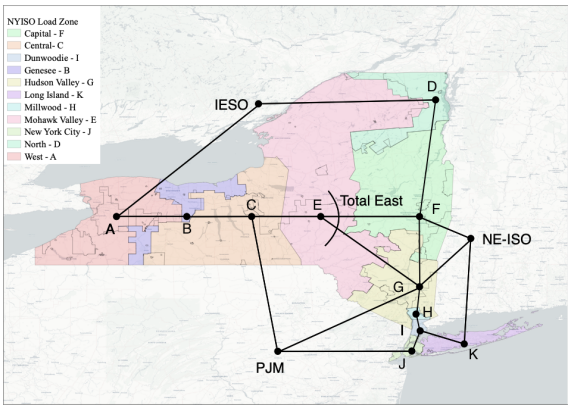


**Figure 1. Connections between load zones and neighbor grids**

### 2.2. Renewable Resources

The renewable resources to be added to the baseline model include land-based and offshore wind, utility-scale solar, and behind-the-meter (BTM) solar. According to the climate change impact phase II report, 17,761 MW of wind, 19,631 MW of utility solar, and 5,440 MW of BTM solar are allocated to each zone as shown in Table 2. The zonal capacity of utility solar and wind is then further dis-aggregated to PV buses (only BTM solar can be included on PQ buses) in the baseline model based on potential wind and solar sites identified by the National Renewable Energy Lab (NREL) Wind

**Table 1. Interface Flow Limits (MW)**

| Interface | Lower Bound | Upper Bound |
|---|---|---|
| A-B | -2,200 | 2,200 |
| B-C | -1,600 | 1,500 |
| C-E | -5,650 | 5,650 |
| D-E | -1,600 | 2,650 |
| E-F | -3,925 | 3,925 |
| E-G | -1,600 | 2,300 |
| F-G | -5,400 | 5,400 |
| G-H | -7,375 | 7,375 |
| H-I | -8,450 | 8,450 |
| I-J | -4,350 | 4,350 |
| I-K | -515 | 1,293 |
| Total East | -3,400 | 5,600 |
| NY-NE | -1,700 | 1,300 |
| NY-IESO | -2,000 | 1,650 |
| NY-PJM | -900 | 500 |

**Table 2. Zonal Capacity Allocation (MW)**

| Zone | Wind | Utility Solar | BTM Solar | Storage |
|---|---|---|---|---|
| A | 2692 | 5748 | 704 | 956 |
| B | 390 | 656 | 218 | 4 |
| C | 1923 | 3585 | 596 | 979 |
| D | 1935 | - | 69 | 988 |
| E | 1821 | 2268 | 673 | 344 |
| F | - | 4661 | 827 | 303 |
| G | - | 1636 | 684 | 84 |
| H | - | - | 61 | - |
| I | - | - | 90 | - |
| J | 6391 | - | 672 | 195 |
| K | 2609 | 77. | 846 | 27 |

Tool Kit (WTK) [14] and Solar Integration National Dataset (SIND) [15], respectively. As a result, 14 wind generators and 14 utility-scale solar sites are added as generators to the baseline model along with 24 BTM solar sites added as negative loads.

The time series trajectories of these synthetic wind and solar sites are then generated using wind speed, incident solar radiation, and ambient air temperature data from MERRA-2 reanalysis data [16]. The data is scaled and bias-corrected following the methodology in [17] to generate hourly wind and solar power for 2019. The spatiotemporal co-variability is well preserved across all the wind and solar sites given the historical data.

### 2.3. Storage Data

The storage capacity of each load zone also follows [7], which is based on the 2019 CARIS Phase I starting point and modified to provide the most efficient "shifting" of renewables across time, resulting in the capacity distribution shown in Table 2. Similar to renewable resources, the zonal capacity needs to be disaggregated for each bus. Batteries are allocated based on the percentage of renewable resources on each bus as well as the congestion pattern. Nodes with a higher concentration of renewables are given higher priority to be assigned to storage units. If there are buses with a similar renewable penetration level, the buses with higher congestion tendencies are prioritized. Battery sizes vary from 4 to 988 MW. Note that, a 988MW battery could be several smaller-sized batteries connected to the same bus in reality. One bus is assumed to have a single battery to reduce computational complexity. The Gilboa pumped hydro is modeled as a 1,170 MW battery in the system. As a result, 20 storage units are allocated to the baseline model. Even though [7] suggested 8-hour battery duration, 2-hour and 4-hour batteries are the most popular ones in the current US markets [18]. We test how different battery durations impact the utilization of renewables in Section 5.4.

## 3. Model and Formulation

To focus on the feasibility of the CLCPA plan and to avoid complexity brought by market bidding strategies, DC-OPF formulation is used to decide the dispatch of generators and the charging/discharging of storage units. This approach assumes that the system operator manages all the resources and aims to satisfy demand and system constraints with the minimum total cost over the optimization horizon. A linear cost function is provided for each generator by the baseline model. To prioritize the dispatch of wind and solar, zero marginal costs are assigned to wind and solar generators, whereas hydro units have a marginal cost of 3 $/MW. A small marginal cost of 1 $/MW is assigned to charging and discharging to encourage the use of batteries while preventing simultaneous charge and discharge. As nuclear units served as base load and operated at maximum capacity for most of 2019, these units are constrained to run at full capacity. The objective function can then be formulated as equation 1

$$\sum_{t=1}^{T}(\sum_{g=1}^{Gn}(C^{c}_{g,t}+C^{1}_{g,t}p_{g,t})+\sum_{s=1}^{S_n}(\delta^{+}_{s,t}+\delta^{-}_{s,t}) \quad (1)$$

The DC-OPF constraints including charging and

discharging can be written as equation 2 to 7

$$\sum_{g\in G_b} p_{g,t} + \sum_{l\in I_b} e_{l,t} + \sum_{s\in S_b} \delta^-_{s,t} = \sum_{l\in O_b} e_{l,t} + D_{b,t} + \sum_{s\in S_b} \delta^+_{s,t}, \forall t \in T, b \in Bn \tag{2}$$

$$\underline{P}_g \leq p_{g,t} \leq \overline{P}_g, \forall t \in T, g \in Gn \tag{3}$$

$$\underline{R}_g \leq p_{g,t} - p_{g,t-1} \leq \overline{R}_g, \forall t \in T, g \in Gn \tag{4}$$

$$\underline{L} \leq e_{l,t} \leq \overline{L}, \forall t \in T, l \in Ln \tag{5}$$

$$-\pi \leq \theta_{b,t} \leq \pi, \forall t \in T, b \in Bn \tag{6}$$

$$e_{l,t} = B_l(\theta_{b,t} - \theta_{b',t}), \forall t \in T, l \in Ln \tag{7}$$

where equation 2 is the power balance constraint, equation 3 and 4 are the power limits and ramping constraints for generators. The thermal generation has a lower bound at zero to approximate the unit commitment process as suggested by [10]. It is worth mentioning that the upper bounds for renewable generators are changing over time based on resource availability. We use the power output derived in Section 2.2 as the upper bound for wind and solar, so that wind and solar generators are semi-dispatchable. This means that the "free" renewable resources can be dispatched at any level lower than or equal to the maximum output determined by the available wind speed or solar radiation. The difference between the dispatched energy and the upper bound of a specific hour is the curtailed or "spilled" wind and solar generation. The hydro plants are assumed to be dispatchable units with a small cost in this study to prioritize the use of wind and solar. In this case, the difference between the generation upper bound and dispatch for hydro is similar to other dispatchable resources, which is the unused capacity of hydro. Equation 5 is the transmission line limit constraint, equation 6 is the phase angle limit constraint and equation 7 is the linearized relationship between the power flow and the phase angle.

As suggested by [7], the batteries are assumed to have round trip efficiency of $\eta = 85\%$ and the Gilboa pumped hydro has round trip efficiency of $\eta = 75\%$. The constraints for batteries can be formulated as:

$$soc_{s,t+1} = soc_{s,t} + \frac{1}{\sqrt{\eta_s}}\delta^+_{s,t} - \sqrt{\eta_s}\delta^-_{s,t} \tag{8}$$

$$0 \leq soc_{s,t} \leq \overline{SOC_s}, \forall t \in T, s \in Sn \tag{9}$$

$$0 \leq \delta^-_{s,t} \leq \Delta_s, \forall t \in T, s \in Sn \tag{10}$$

$$0 \leq \delta^+_{s,t} \leq \Delta_s, \forall t \in T, s \in Sn \tag{11}$$

where equation 8 is the State-Of-Charge (SOC) transition constraints, equation 9 is the storage size limit constraint and $\overline{SOC_s} = k\Delta_s$. $k$ is the battery duration and will be analyzed in Section 5.4. Equation 10 and 11 are the limit constraints for discharging and charging.

NYISO specifies interface flow limits between load zones and neighboring areas, which constrain the amount of energy that can be transferred through a group of lines connecting two areas/zones. The interface flow constraints can be formulated as equation 12

$$\underline{L_{IF_i}} \leq \sum_{l\in IF_i} e_{l,t} \leq \overline{L_{IF_i}}, \forall t \in T, i \in Ifn \tag{12}$$

The final optimization problem can then be formulated as:

$$\begin{aligned} &\min \quad (1) \\ &s.t. \quad (2) - (12) \end{aligned}$$

## 4. Test Cases

The optimization problem formulated in Section 3 is solved every 24 hours for 365 consecutive days, where sequential days are connected by battery states. To test how the CLCPA plan carries out and to set the groundwork for the complex 2040 scenarios, we set up the following test cases as described in Table 3:

**Table 3. Description for Test Cases**

| Test cases | Description |
|---|---|
| Case 1 | Run DC-OPF with the baseline model without any modification with 2019 load and transmission conditions. |
| Case 2 | Install virtual wind and solar capacities with the time series data described in Section 2.2 while constraining the external areas to generate at the level of 2019. |
| Case 3 | Renewable settings as in test case 2, removing the constraint for generation in external areas |
| Case 4 | Add 8-hour batteries as suggested by [7] to test case 3 with the capacity allocated in Section 2.3 |

The four test cases are designed to progressively achieve the CARIS starting point and ensure that the test cases are comparable. Test case 1 is the baseline case that reflects the historical condition of the year 2019 for all the other test cases to compare. Test case 2 holds the generation condition for neighboring areas as they were in 2019 so that NYS continues to import energy from the external areas. Such a setting imitates a lower bound (for load level) of the future scenario where

the neighboring grids have a similar level of renewable penetration, enabling NYS to continue importing energy much of the time. Test case 3 relaxes the constraints on external generators and serves as an upper bound (as the external areas generate less, NYS will export energy and thus increase the overall load level) of the future scenarios where the neighboring grids do not have as much as renewable as NYS and will tend to import less expensive energy from NYS. Note that test cases 2 and 3 do not have storage units. In case 4, 8-hour batteries are added to test case 3 to analyze how much flexibility storage units can provide. Note that, the four cases use historical load and projected renewable outputs as perfect forecasts, which provides a lower bound for the minimized objective function (equivalent to the upper bound of system performance).

# 5. Numerical Results

We start with an annual overview (Section 5.1) and then highlight daily results over the year (Section 5.2) to discuss seasonal variations. A specific day will then be analyzed as an example in Section 5.3 followed by battery duration analysis in Section 5.4

## 5.1. Annual Overview

The comparison of generation composition for the full year is shown in Table 4 for the four test cases. The result of test case 1 is aligned with the historical generation in 2019 [19], where approximately 40% of the energy is from thermal generators. Compared to case 1, cases 2 and 3 significantly reduce the usage of thermal from 38.15% to 12.05% and 11.43% while using 52% and 63% of renewable generation, which are under the 70% goal set by the 2019 CARIS report [8]. Recall that in test case 3, NYS exports energy to neighboring grids because the overall generation in NYS is less expensive. As a result, test case 3 has a higher generation level than case 2, which reduces the percentage of the nuclear composition. With 8-hour batteries to shift the energy in case 4, an extra 2% of renewables can be used compared to case 3.

We quantify the unused wind, solar, and hydro in Table 5 to highlight that the current grid cannot take full advantage of the planned renewable resources. Table 5 will be of particular relevance in Section 5.3 where we observe the use of thermal units in lieu of cleaner and less expensive hydro generation. Another observation is that, from case 2 to case 4, since there is no cost to dispatch wind and solar, the quantity of unused wind and solar declines first followed by hydro. It is also as expected that case 3 consumes more renewables due to the relaxation of constraints for external generators. Last but not least, it is worth noting that even with batteries included in case 4, there's still unused capacity of hydro while thermal resources continue to provide around 10% of the total. We look into finer time intervals in Section 5.2 and 5.3 to investigate potential causes of such results.

**Table 4. Fuel Mix of four test cases**

| Fuel Type | Case1 | Case2 | Case3 | Case4 |
|---|---|---|---|---|
| thermal | 38.15% | 12.05% | 11.43% | 9.98% |
| Nuclear | 32.96% | 35.61% | 25.39% | 25.06% |
| Hydro | 25.79% | 7.50% | 14.30% | 15.41% |
| Wind | 3.10% | 31.83% | 34.42% | 34.54% |
| Solar | NA | 13.00% | 14.45% | 15.01% |

**Table 5. Unused Renewable four test cases**

| Renewable Type | Case1 | Case2 | Case3 | Case4 |
|---|---|---|---|---|
| Wind | NA | 37.23% | 2.65% | 1.01% |
| Solar | NA | 41.80% | 7.24% | 0.02% |
| Hydro | NA | 73.79% | 28.39% | 21.79% |

## 5.2. Daily Overview

To explore the dynamic pattern of the system behavior, the aggregated daily generation composition and unused renewable for case 4 are plotted for the whole year in Figure 2. Case 4 is chosen as an illustration here because it utilizes the renewables with batteries most efficiently. The upper panel of Figure 2 shows the generation by fuel type in different colors where charging is plotted as a negative value to distinguish from discharging. Load is denoted as the thick black line, which verifies the exportation of power to neighboring areas as the total generation is consistently higher than the load. The lower panel shows the curtailed wind, solar and hydro aggregated for each day.

In general, summer brings reductions in curtailment and increases in thermal usage (in orange) due to the lack of wind, which matches the seasonal wind generation pattern recorded by NYISO [12]. Conversely, more curtailment and reduced thermal usage are observed in the shoulder seasons because demand is lower and the wind resources exhibit higher capacity factor during spring and fall seasons. Note that thermal units continue to be used nearly every day throughout the year, indicating a lack of renewables during certain hours of the day, transmission line congestion, or insufficient energy shifting capability from batteries. To understand these challenges, we next more closely examine the intra-day behavior under this high renewable level scenario.

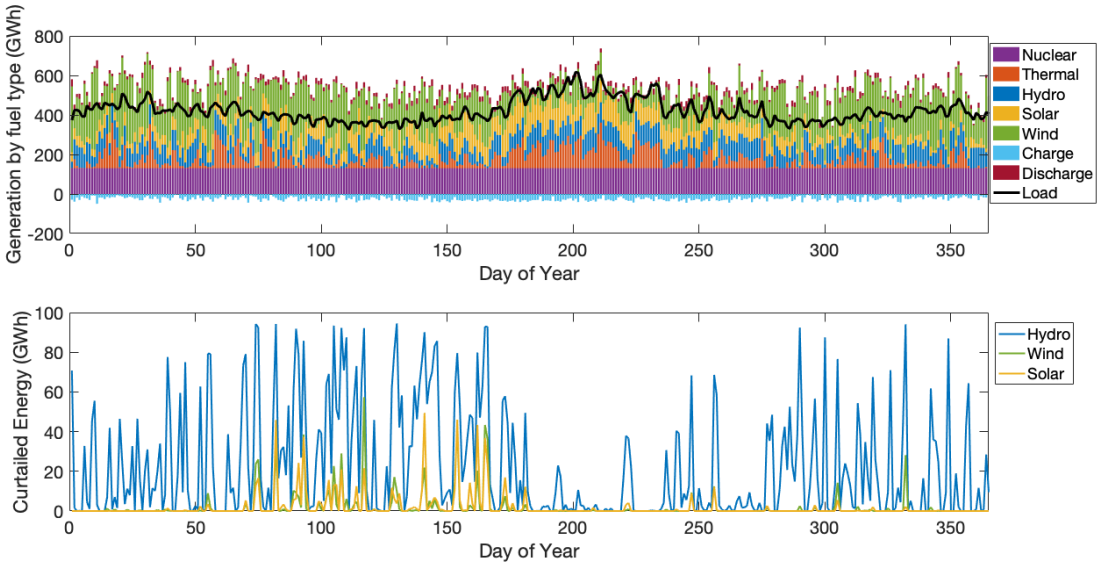


**Figure 2. Daily Overview for case4**

## 5.3. Intra-Day Analysis

A single day (Apr 27, 2019) with high curtailment of wind, solar, and unused capacity of hydro, is presented to investigate the diurnal dynamics of the system. As shown in Figure 3, the upper panel is the generation composition and the lower panel shows the renewable resource curtailments. Hydro is consistently not used throughout the day as it has higher cost than wind and solar. The batteries are charged in the middle of the day when excess "free" wind and solar generation are available. At hour 17, the curtailment of wind and solar power reduces to zero, and hydro power is added to the generation mix along with some thermal units. Batteries discharge as the thermal generators are turned on to take advantage of the energy that was stored earlier in the day.

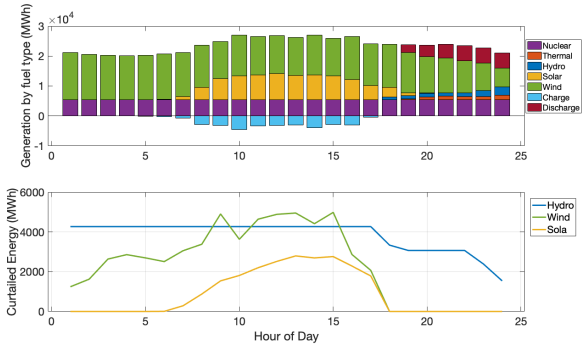


**Figure 3. Generation composition and renewable curtailment of Apr 27, 2019.**

Towards the end of the day, hydro units get dispatched but there is still significant amount of extra hydro power available, even while thermal units are brought online. To investigate the underlying reason, the interface flows between each load zone and NYS-to-neighboring areas are shown in Figure 4 and the Locational Marginal Prices (LMPs) for each zone are shown in Figure 5. The blue lines in Figure 4 indicate the temporal interface flows, the orange lines denote the interface flow limits, and the vertical red lines highlight hour 17, which is the transition from the period of excess renewable resources to the use of thermal units. Similarly, Figure 5 includes the vertical red lines to highlight this transition hour. It should be emphasized that the LMPs in all the load zones increase after the transition hour. However, in load zone A-E, the LMPs are within the range $2 - 3\$/MW$ indicating hydro power is on the margin, while zone F-K shows LMPs are near $20\$/MW$, indicating a thermal unit is on the margin. This observation suggests that upstate zones (A-E) have extra hydro power that cannot be transferred to downstate zones (F-K), which can further be verified by Figure 4: note that D-E and Total East (which is E-F plus E-G) are both at maximum capacity when the thermal units are on, implying that there is no extra capacity to transfer power from upstate to downstate. As a result, the hydro power (noting that most of the NYS hydro power exists in zone A and D) are not being used while downstate areas need to turn on thermal generators to satisfy demand. To summarize, even on a day with excess renewables, thermal units are still necessary due to the imbalance in load and

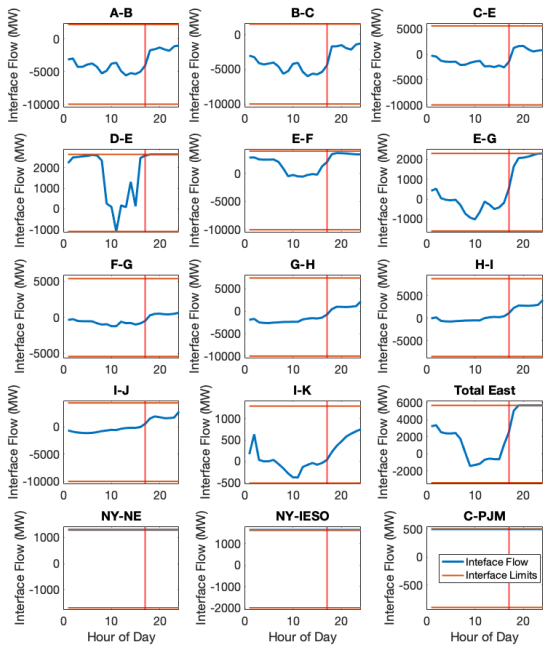


**Figure 4. Interface flows between load zones and neighboring areas**

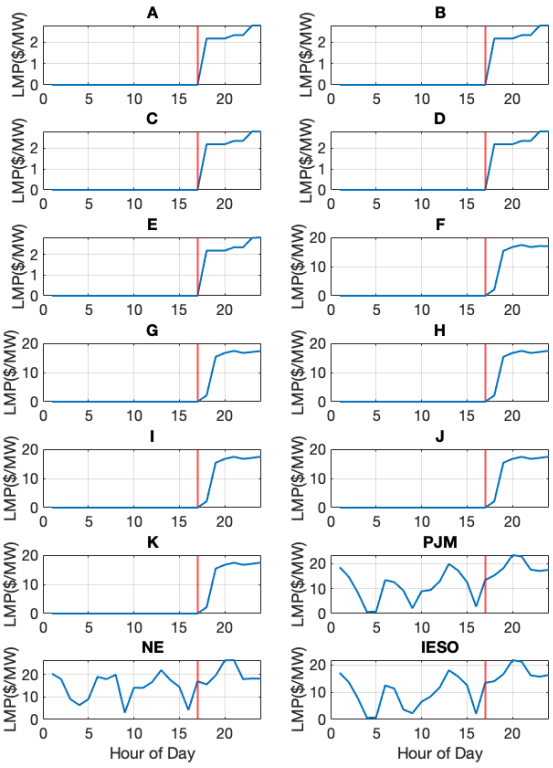


**Figure 5. LMPs of each load zone and neighboring areas**

renewable distribution between upstate and downstate zones, implying insufficient transmission line capacity expansion.

To demonstrate the congestion pattern of the system, the generation condition of each zone and the transmission condition of each interface for hour 16 and hour 20 are presented in Figures 6 and 7. For both figures, black circles indicate that there is no curtailment or thermal units on, black diamonds show that hydro is being curtailed in that zone, and green diamonds denote wind and/or solar curtailment (indistinguishable, as wind and solar both have zero marginal cost) and unused capacity of hydro. The orange circles indicate that there are thermal generators on in that zone. Red transmission lines indicate that the interface is at capacity, whereas blue lines indicate free capacity, and the thickness of the line indicates the percentage of usage for that interface (i.e. a thin blue line indicates lowest line usage). Figure 6 shows that in hour 16, the path from upstate zones to downstate zones still has capacity so there are no thermal units on. Whereas in Figure 7 we can see that in hour 20, there no longer exists a feasible path from upstate to downstate as E-F and E-G transfer constraints are binding so that zones F and J cannot receive extra renewables and require thermal generation to meet load requirements. In fact, the congested area is highly concentrated at E-F and E-G throughout the year, suggesting that more transmission capacity is needed for this critical area.

Another key observation is that the batteries are not being fully used throughout the day. Recall that 8-hour batteries are used in this test case, which means the batteries should be able to discharge at full capacity for 8 hours. However, only 6 hours of discharge is observed by the end of the day, which raises the question of whether 8-hour batteries are necessary given that 2-hour and 4-hour batteries are the most established types in the current market. To answer this question, we perform a battery duration analysis in the next section.

## 5.4. Battery Analysis

Batteries are critical resources that provide flexibility in the power grids to use renewable energy more efficiently. Currently, in the power markets, 2-hour and 4-hour batteries are most commonly used, so one key focus of this section is to investigate the impact of battery duration on the use of renewable energy. Another practical concern for batteries is the cycling constraints, which restrict the battery to operate one cycle a day to prevent rapid degradation. The battery is considered to have gone through one cycle when it has fully discharged its storage capability (i.e. capacity multiplied by duration), which can be formulated as

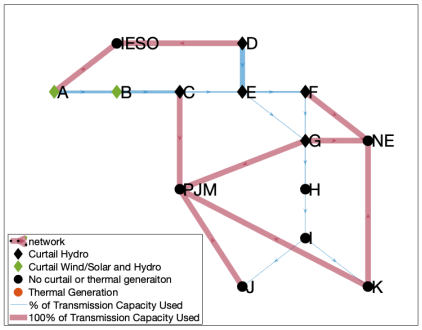


**Figure 6. System condition of hour 16.**

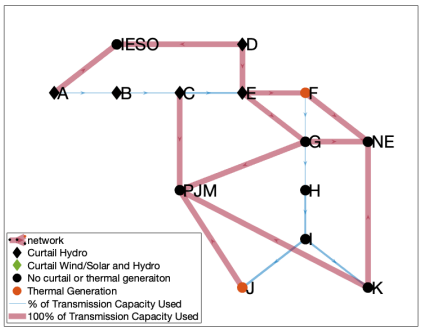


**Figure 7. System condition of hour 20.**

equation 13

$$\sum_{t=1}^{T} \delta_{s,t}^{-} \leq \overline{SOC_s}, \forall t \in T, s \in Sn \tag{13}$$

The following six test cases are designed to analyze how different duration configurations and the cycling constraint can impact the system behavior:

- Case 1: 2-hour battery with cycling constraints
- Case 2: 2-hour battery without cycling constraints
- Case 3: 4-hour battery with cycling constraints
- Case 4: 4-hour battery without cycling constraints
- Case 5: 8-hour battery with cycling constraints
- Case 6: 8-hour battery without cycling constraints (This is the same as Test Case 4 in Section 4)

Note that in the real power system, it is not realistic to have only one configuration of battery duration. The test cases here serve as three checkpoints to bound the impact of the batteries, and we can assume that the combination of different duration configurations would give results in between these bounds. We compare the level of thermal and renewable usage of each case, as well as the average battery cycles over the year in Table 6.

**Table 6. Comparison for battery configurations**

| Test Case | thermal GWh | Renewable GWh | Battery Cycles |
|---|---|---|---|
| Case1 | 19,767 | 121,980 | 333.5 |
| Case2 | 19,679 | 122,047 | 412.7 |
| Case3 | 19,235 | 122,839 | 305.9 |
| Case4 | 19,203 | 122,877 | 330.4 |
| Case5 | 18,949 | 123,313 | 220.2 |
| Case6 | 18,943 | 123,316 | 221.6 |

By comparing cases with and without cycling constraints, the differences in thermal and renewable balance tend to decrease as the battery duration increases. Specifically, with 8-hour batteries, the difference between constrained and unconstrained cycling is only $6GWh$ of thermal generation over the entire year. This result verifies that 8-hour batteries may be excessive for the system, assuming the system operates at the daily horizon. In other words, there are not many opportunities to charge and discharge batteries of this capacity within a day. This might be counter-intuitive at the first glance, but recall that the batteries are assumed to be owned by the system operator and are operated to minimize the overall generation cost. This is as opposed to the case that the batteries are actively bidding in the system to maximize their profits, which would lead to different use patterns. Within this configuration, 2-hour batteries see the largest impact of the cycling constraint, though even the 2-hour batteries only operate 1.13 cycles on average each day *without* the cycling constraints. This small difference suggests that the cycling constraints should be considered in operations to prevent fast degradation of batteries, since this will have a significant impact on overall system efficiency.

Another observation is that as battery duration increases, the amount of thermal generation decreases, and the amount of renewable generation increases. As longer duration gives the battery a larger storage size and more flexibility to shift the excessive renewable generation to peak load hours, it is reasonable to see the 8-hour batteries supporting the use of more renewable energy. As for future planning, if the batteries are operated daily, it may not be economically efficient use 8-hour batteries as suggested by [7]. Based on Table 6, the reduction in thermal generation is only approximately 200 GWh for the full year, indicating that

the 4-hour duration batteries can satisfy the need for most situations. However, this is not to underestimate the need for other technologies to enable energy storage for the long term (for example between seasons). Figure 2 and [7] show that shoulder seasons have more excess renewables to be shifted to winter and summer seasons and strategies to reduce curtailment and take advantage of this low-cost and low-emissions energy should be considered in the future.

## 6. Future work and Conclusion

In this paper, the starting configuration proposed in the CLCPA is simulated over the entire year of 2019 to investigate the feasibility of the plan. Taking advantage of the high-resolution spatial-temporal historical data, the co-variability of renewable output and load can be properly considered. However, it should be emphasized that by using the 2019 data, the effect of climate change for 2030 and the load increase due to proposed electrification (potentially shifting from summer peak to winter peak) and/or climate impacts on temperature are not considered. The simulation result is implemented under a milder condition, treating historical data as perfect forecasts. Compared to the projected 2030/2040 scenario, the result presented here can serve as an upper bound estimate of system performance. Even under these milder conditions, the goal of 70% renewable generation is barely achievable. Transmission capability from upstate to downstate is one of the critical bottlenecks that is limiting the effective use of renewable resources. The "Total East" interface is identified to have the highest congestion probability and more attention should be paid to alleviating the congestion in this area.

Furthermore, the potential flexibility to shift renewable energy provided by storage units is studied. The 3,900 MW of storage proposed in the CLCPA can increase renewable usage by 2% with 8-hour batteries. Our results show that the cycling constraint of batteries is not a significant factor, so it is likely more economically and environmentally efficient to adhere to the cycling constraint and prolong the life span of batteries. In addition, the duration of batteries needs to be carefully considered. The results of this analysis indicate that the ideal duration is around 4 hours for daily operations as 8-hour batteries are not fully utilized for most days, and 2-hour batteries would require extra cycles leading to faster degradation. To use renewable energy more efficiently, a larger capacity of batteries is needed. Meanwhile, testing longer operation horizons for batteries, i.e. instead of running daily operation, a weekly operation horizon might highlight the benefits of longer-duration batteries. Technologies and mechanisms to store the excess energy in shoulder seasons for use in peak load months could be valuable resources to improve the overall system efficiency.

This research can be extended in the future with more attention paid to hydro resources, as it accounts for over 20% of annual generation in the current system. The correlation between hydro power and other variables in the system such as wind, solar, and load should be properly modeled. It would also be interesting to study the worst-case scenarios and understand how long-term climate change could impact load patterns, renewable outputs, and transmission line limits. In addition, the nuclear units are gradually retiring, with two nuclear generators already offline in 2020. Therefore, given the social and political concerns surrounding this resource, a future test scenario should consider the retirement of all the nuclear units, and the impact of this decision on decarbonization goals and grid performance. Understanding the correlation between climate factors and the system behavior is of great importance to transition to the next generation of power grids efficiently and reliably. Overall, this paper provides a practical exploration of the CLCPA plan based on historical data for NYS and could serve as a solid foundation for more in-depth research of the pathway to a zero-emission grid.

## References


[1] V. Masson-Delmotte, P. Zhai, A. Pirani, S. L. Connors, C. Péan, S. Berger, N. Caud, Y. Chen, L. Goldfarb, M. Gomis, *et al.*, "Climate change 2021: the physical science basis," *Contribution of working group I to the sixth assessment report of the intergovernmental panel on climate change*, p. 2, 2021.

[2] M. Ge, J. Friedrich, and L. Vigna, "4 charts explain greenhouse gas emissions by countries and sectors." https://thecityfix.com/blog/4-charts-explain-greenhouse-gas-emissions-countries-sectors. Accessed: 2022-06-08.

[3] K. Sun, H. Xiao, S. Liu, S. You, F. Yang, Y. Dong, W. Wang, and Y. Liu, "A review of clean electricity policies—from countries to utilities," *Sustainability*, vol. 12, no. 19, p. 7946, 2020.

[4] M. Z. Jacobson, M. A. Delucchi, G. Bazouin, Z. A. F. Bauer, C. C. Heavey, E. Fisher, S. B. Morris, D. J. Y. Piekutowski, T. A. Vencill, and T. W. Yeskoo, "100% clean and renewable wind{,} water{,} and sunlight (WWS) all-sector energy roadmaps for the 50 United States," *Energy Environ. Sci.*, vol. 8, no. 7, pp. 2093–2117, 2015.

[5] N. Zhao and F. You, "Toward Carbon-Neutral Electric Power Systems in the New York State: a Novel Multi-Scale Bottom-Up Optimization Framework Coupled with Machine Learning for Capacity Planning at Hourly Resolution," *ACS Sustainable Chemistry & Engineering*, vol. 10, no. 5, pp. 1805–1821, 2022.

[6] Itron, "New York ISO Climate Change Impact Study Phase 1 : Long-Term Load Impact," vol. 02116, no. December, 2019.

[7] P. J. Hibbard, "Climate Change Impact Phase II An Assessment of Climate Change Authors :," 2020.

[8] New York Independent System Operator, "Congestion Assessment and Resource Integration Studies," 2018.

[9] New York Independent System Operator, "NYISO Gold Book - Load and Capacity Data," p. 113, 2019.

[10] M. V. Liu, B. Yuan, Z. Wang, J. A. Sward, K. M. Zhang, and C. L. Anderson, "An open source representation for the nys electric grid to support power grid and market transition studies," *IEEE Transactions on Power Systems (In Press)*, 2022.

[11] New York Independent System Operator, "NYISO Gold Book - Load and Capacity Data," p. 139, 2022.

[12] New York Independent System Operator, "New York ISO — Energy and Market Operational Data." https://www.nyiso.com/energy-market-operational-data. Accessed: 2022-04-28.

[13] New York Independent System Operator, "2020 Reliability Needs Assessment," 2020.

[14] C. Draxl, A. Clifton, B.-M. Hodge, and J. McCaa, "The wind integration national dataset (wind) toolkit," *Applied Energy*, vol. 151, pp. 355–366, 2015.

[15] A. Bloom, A. Townsend, D. Palchak, J. Novacheck, J. King, C. Barrows, E. Ibanez, M. O'Connell, G. Jordan, B. Roberts, *et al.*, "Eastern renewable generation integration study," tech. rep., National Renewable Energy Lab.(NREL), Golden, CO (United States), 2016.

[16] A. Molod, L. Takacs, M. Suarez, and J. Bacmeister, "Development of the geos-5 atmospheric general circulation model: Evolution from merra to merra2," *Geoscientific Model Development*, vol. 8, no. 5, pp. 1339–1356, 2015.

[17] K. Doering, C. L. Anderson, and S. Steinschneider, "Evaluating the intensity-duration-frequency behavior of energy deficits in a zero-emission, hydropower reliant power system," *To be submitted*, 2022.

[18] C. Augustine and N. Blair, "Storage futures study: Storage technology modeling input data report," tech. rep., National Renewable Energy Lab.(NREL), Golden, CO (United States), 2021.

[19] New York Independent System Operator, "NYISO Gold Book - Load and Capacity Data," p. 139, 2020.